American Journal of Pathology, Vol. 158, No. 1, January 2001

Technical Advance

Three-Dimensional Imaging of Embryonic Mouse Kidney by Two-Photon Microscopy

Carrie L. Phillips,* Lois J. Arend,† Adele J. Filson,* Doug J. Kojetin,* Jeffrey L. Clendenon,* Shiaofen Fang,‡ and Kenneth W. Dunn*

From the Department of Medicine, Division of Nephrology, Indiana University School of Medicine, Indianapolis, Indiana; the Department of Pathology and Laboratory Medicine,† University of Rochester Medical Center, Rochester, New York; and the Department of Computer and Information Science,‡ Indiana University-Purdue University at Indianapolis, Indianapolis, Indiana*

Developing mammalian embryonic kidney becomes progressively more elaborate as the ureteric bud branches into undifferentiated mesenchyme. Morphological perturbations of nephrogenesis, such as those seen in inherited renal diseases or induced in transgenic animals, require careful and often tedious documentation by multiple methodologies. We have applied a relatively quick and simple approach combining two-photon microscopy and advanced three-dimensional (3-D) imaging techniques to visualize and evaluate these complex events. As compared with laser confocal microscopy, two-photon microscopy offers superior optical sectioning deep into biological tissues, permitting analysis of large, heterogeneous, 3-D structures such as developing mouse kidney. Embryonic and newborn mouse kidneys were fluorescently labeled with lectins, phalloidin, or antibody. Three-dimensional image volumes were then collected. The resulting volume data sets were processed using a novel 3-D visualization technique. Reconstructed image volumes demonstrate the dichotomous branching of ureteric bud as it progresses from a simple, symmetrical structure into an elaborate, asymmetrical collecting system of multiple branches. Detailed morphology of *in situ* cysts was elucidated in a transgene-induced mouse model of polycystic kidney disease. We expect this integration of two-photon microscopy with advanced 3-D image analysis will provide a powerful tool for illuminating a variety of complex developmental processes in multiple dimensions. ***(Am J Pathol 2001, 158:49–55)***

The study of biological development has been furthered by recent advances in molecular biology. For example, transgenic animal models allow for the selective expression of genes, permitting analysis of developmental consequences of specific mutations. *In vivo* expression of chimeric green fluorescent proteins fused to specific recombinant proteins permit the analysis of spatio-temporal protein distribution. Nonetheless, our understanding of development is still confounded by the inherent three-dimensional (3-D) complexity of tissues and organs. Developmental processes are difficult to evaluate by conventional histological approaches. Though 3-D data may be assembled from serial tissue sections, the process is laborious and the resulting image volumes are difficult to analyze.

Laser confocal microscopy rapidly captures optical sections, thereby offering a relatively quick method for generating 3-D image volumes from fluorescently labeled tissues. When originally introduced, this potential was hampered by the lack of microscope objectives capable of collecting image volumes more than a few microns thick. Water immersion objectives with longer working distances now give confocal microscopes the potential to collect image volumes up to hundreds of microns in thickness.[1–3] In practice, however, significant light scattering in biological tissues limits the depth of confocal imaging. This problem has, in turn, been addressed with the development of two-photon microscopy, a method of optical sectioning that dispenses with the confocal aperture and, thus, more efficiently collects scattered fluorescence.[4] Two-photon microscopy now offers the ability to image biological structures whose size is on the scale of millimeters with submicron resolution.

Supported by National Kidney Foundation of Indiana, Indiana University School of Medicine Biomedical Research Grant, Clarian Health Values Fund VFR21, Polycystic Kidney Research Foundation 99023 (to C. P.), National Institutes of Health grant K08 DK02515, Amgen Young Investigator Grant of the National Kidney Foundation (to L. A.), and the Indiana University Strategic Directions Initiative (to K. D. and S. F.).

Accepted for publication September 21, 2000.

Address reprint requests to Carrie L. Phillips, Indiana University School of Medicine, Department of Medicine, Division of Nephrology, 1120 South Drive, Fesler Hall 115, Indianapolis, IN 46202-5116. E-mail:sphilli3@iupui.edu.

Evaluation of data sets is complicated by the difficulty of analyzing cubic image volumes. First, the size of the digital image volumes with this kind of scale and resolution may exceed 50 to 100 megabytes, imposing huge processing requirements for data handling and analysis. Second, the three-dimensionality of such data is lost in 2-D image displays and printouts. While there has been an explosive development of digital image technology in computer gaming, multimedia, and even medical imaging, very little of this technology has been applied to analysis of microscopy image volumes. In this report, we use novel image processing tools specifically designed for analysis of microscopy image volumes.

The present study offers a new methodology to assess morphology and function of developing mouse kidney using a combination of two-photon microscopy and advanced image processing techniques. Development of mammalian kidney is particularly intriguing because nephrogenesis involves the reciprocal induction of two distinct embryonic tissues: the Wolffian duct-derived ureteric bud and the metanephrogenic mesenchyme. In the mouse, nephrogenesis begins at embryonic day 11 and is still apparent in newborn kidneys.[5] The ureteric bud branches to form the urinary collecting system, while the mesenchyme divides and differentiates into nephric epithelia (nephrons) or stroma.[5] Careful reconstruction of serial histological sections,[6,7] scanning electron microscopy,[8] and microdissection of individual nephron segments[9–13] are established methods of reassembling 3-D events of nephrogenesis.

Two-photon microscopy permits *in situ* analysis of protein distribution while simultaneously defining 3-D tissue microstructure. Therefore, we stained kidneys with fluorochrome-conjugated lectins, phalloidin, or Tamm-Horsfall antibody. Lectins were chosen because these sugar-binding proteins can reproducibly bind to and discriminate between the developing kidney structures.[14] Phalloidin serves as a molecular marker for filamentous actin (F-actin). Tamm-Horsfall protein is produced by thick ascending loop of Henle and serves as a marker of the distal nephron.[15] Morphological analysis was performed on kidneys from normal embryonic and newborn mice and transgenic *inv* mice with polycystic kidney disease (PKD). Mice homozygous for inversion of embryonic turning (*inv/inv*) have polycystic kidneys[16] and, as such, were used to demonstrate the power of two-photon microscopy in establishing morphology of *in situ* cyst formation.

Materials and Methods

Animals and Tissue Procurement

Handling, care, and euthanasia of mice conformed to institutional animal care guidelines. After euthanasia, kidneys were harvested from embryonic (E) or early postpartum (P) mice and placed in 4% paraformaldehyde/1× phosphate buffered saline (PBS; Fisher Scientific, Fair Lawn, NJ) for overnight fixation. Conditions were as follows:

Normal embryonic kidneys were obtained from timed pregnant CD-1 female mice (Harlan, Indianapolis, IN). Pregnancy was dated using presence of vaginal plug as embryonic day (E) 0.5. Embryonic kidneys were dissected on E11.5 , E13.5, and E17.5.

Postpartum day 5 (P5) kidneys were obtained from OVE210 *inv* mice (inversion of embryonic turning, provided by Paul Overbeek, Baylor College of Medicine, Houston, TX).

Fluorescence Labeling

Kidneys were removed from paraformaldehyde and washed in 1× PBS for 4 hours at room temperature. Kidneys of newborn mice (P5) were vibratome-sectioned (40–180 μm thick). Embryonic kidneys were processed without vibratome sectioning. Tissues were incubated overnight (4°C) with one of the following: fluorescein-phalloidin (Molecular Probes, Eugene, OR), fluorescein-soybean agglutinin, rhodamine-*Dolichos biflorus*, rhodamine- or fluorescein-*Lens culinaris*, rhodamine- or fluorescein-peanut agglutinin (Vector Labs, Burlingame, CA), or Tamm-Horsfall antibody (Biomedical Technologies Inc., Stoughton, MA).

The lectin peanut agglutinin (PNA) stains ureteric bud, collecting duct, and proximal tubule. *Dolichos biflorus* (DBA) and soybean agglutinin (SBA) stain collecting duct and ureteric bud. *Lens culinaris* agglutinin (LCA) binds sugars in mesenchymal, tubular, and vascular structures. Phalloidin (790 daltons) is a bicyclic peptide that stains F-actin. Tamm-Horsfall glycoprotein is expressed in thick ascending loop of Henle.[15] Fluorescein-goat anti-rabbit was used as secondary antibody (Jackson ImmunoResearch Laboratories, West Grove, PA). Lectins, phalloidin, and antibodies were diluted 1:200 in a solution of 2% bovine serum albumin, 0.1% Triton-X 100, and 1× PBS. After a 4-hour wash in 1× PBS, tissue was mounted as follows: (i) vibratome sections were placed in 1× PBS on glass slides with glass coverslips and sealed with clear nail polish and (ii) embryonic kidneys were placed in glass bottom No. 1.5 culture dishes (MatTek Corp., Ashland, MA) with tissue held in place by a lid of cooled 1% agarose (Fisher Scientific).

Two Photon Microscopy

Two-photon microscopy was performed using a BioRad MRC1024 confocal/2 photon system (BioRad, Hercules, CA) fitted to a Nikon Eclipse inverted microscope with a 60×-water immersion, NA 1.2 objective (Nikon, Melville, NY). The thickness of individual coverslips was measured by micrometer, and the objective adjusted accordingly before imaging of each sample. Illumination was provided by a Spectra-Physics (Mountain View, CA) Tsunami Lite Titanium-Sapphire laser tuned to a wavelength of 820 nm. Data sets were collected as Z-series of 200 to 400 images with a spacing of 0.4 μm.

Image Analysis

Real time rendering was performed using Interactive Visualization and Imaging Environment (IVIE) software de-

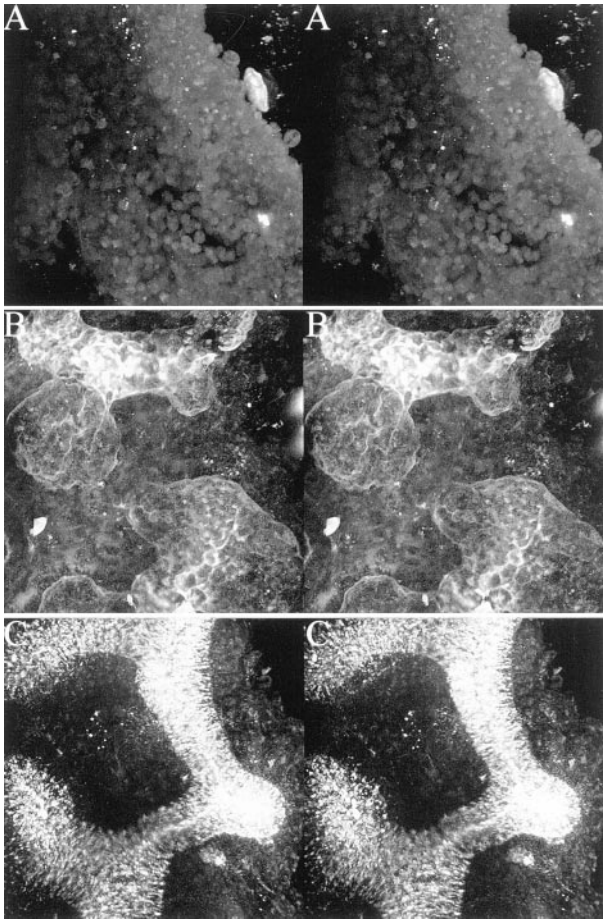

Figure 1. Stereopairs of developing embryonic kidneys imaged by two-photon microscopy. Whole kidneys were microdissected from wild-type mouse embryos, stained with fluorescently conjugated lectins, and imaged by two-photon microscopy. Three-dimensional image processing reveals weak staining of undifferentiated mesenchyme in an E11.5 metanephric rudiment stained with rhodamine-PNA (**A**). By day E13.5, the simple, dichotomously branching ureteric bud is noted to have a cobblestone surface when stained with rhodamine-PNA (**B**) and a spiculated internal structure when stained with fluorescein-SBA (**C**). Each image is 205 μm across. **A** shows projections collected over a depth of 68 μm, **B** a depth of 74 μm, and **C** a depth of 116 μm. These and all subsequent stereopairs are also reproduced as rotating projections located at http://renal.nephrology.iupui.edu/phillip setal.

veloped at Indiana University-Purdue University at Indianapolis. The IVIE software provides volume rendering at speeds of 4 to 8 frames per second for 256 $\times$ 256 $\times$ 256 pixel image volumes. Currently in prototype, this software provides for color manipulations, zooming, 2-D and 3-D image processing tools, and animation making tools. The image volume animations shown here were generated at 8 frames per second using a Silicon Graphics Octane/SE workstation with one 270 MHz R12000 processor, 256 MB of RAM, and 4 MB of texture memory. Satisfactory results may be obtained with lower end Silicon Graphics O2 workstations, and the software is currently being ported to PCs running Windows 2000. The rendering shown in Figure 4 was produced using the PC version of this software, written in C++, and using OpenGL to control an NVIDIA GeForce2 graphics processor (NVIDIA Corp., Santa Clara, CA) on the video board. The program renders each set of images in back-to-front order, combining them using the "over" blending operator and a nonlinear opacity function. Other examples and details can be seen at http://www.cs.iupui.edu/arvl/volume. Stereopairs, rotating animations, and 2-D images were prepared using Metamorph (Universal Imaging, West Chester, PA), Premiere (Adobe, Mountain View, CA), and Photoshop (Adobe) software. Scale bars have been omitted from stereopairs, as they interfere with stereo image formation.

Results

We have combined two-photon microscopy with 3-D image analysis to evaluate the development of normal and cystic kidneys. The image volume data are represented in three forms. First, each image volume is presented as a stereopair, constructed by projecting the image volumes from two different angles. The stereoscopic images

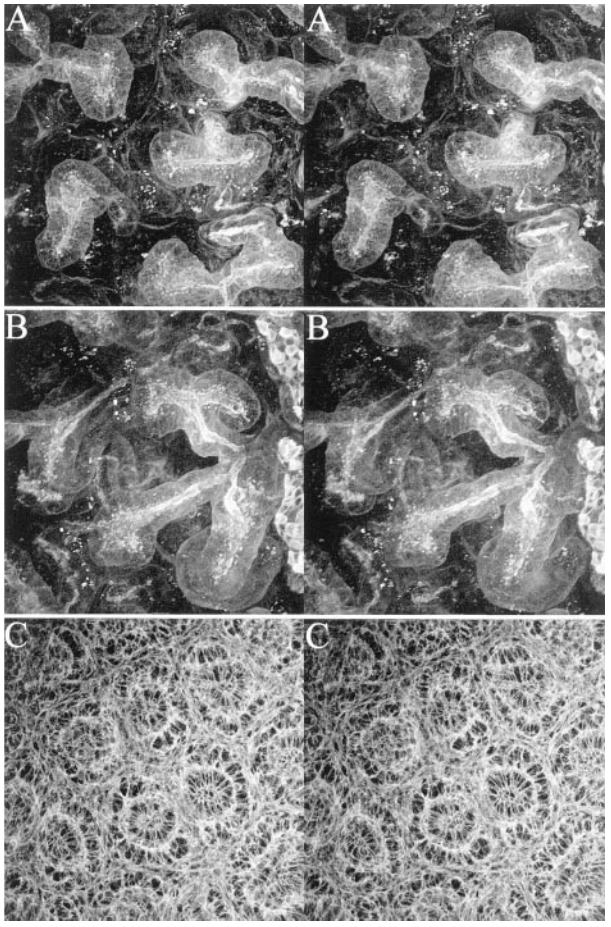

Figure 2. Stereopairs of embryonic day 17.5 kidneys imaged by two-photon microscopy. E17.5 wild-type kidneys were microdissected and labeled with fluorescein-tagged PNA (**A** and **B**) or fluorescein-phalloidin (**C**) to illustrate branches of ureteric bud surrounded by differentiating mesenchyme. PNA shows intense staining of ureteral bud branches and ampullary tips but weakly stains mesenchyme undergoing conversion to epithelial structures (**A** and **B**). After phalloidin staining, this condensed mesenchyme can be seen adjacent to the circular cross sections of ureteric bud (**C**). Careful inspection of **A** and **B** reveals the emergence of faintly staining tubule segments that bridge between the developing nephrons and the ampullae. Each image is 205 microns across. **A** shows projections collected over a depth of 139 μm, **B** a depth of 137 μm, and **C** a depth of 16 μm.

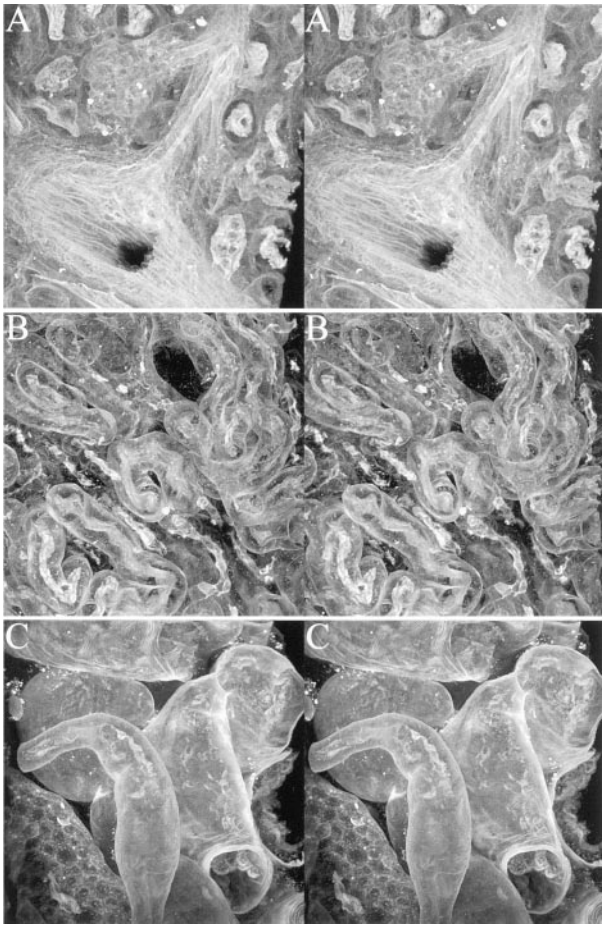

Figure 3. Stereopairs of newborn mouse kidneys imaged by two-photon microscopy. Vibratome sections of P5 kidneys incubated with rhodamine-conjugated lectins LCA (**A**) or PNA (**B** and **C**). **A** shows a normal arcuate artery giving off an interlobular artery which has two afferent arterioles with attached glomeruli. **B** shows normal proximal tubules and scattered collecting ducts with apical labeling of intercalated cells. **C** shows cystic proximal tubules from an *inv/inv* mouse. Compare the cystic collecting duct of **C** (**lower left corner**) to those in **B**. Each image is 205 microns across. **A** shows projections collected over a depth of 100 μm, **B** a depth of 77 μm, and **C** a depth of 130 μm.

may be viewed with a stereo viewer. Alternatively, the two images may be fused into a 3-D image either by crossing one's eyes or by focusing to an infinite distance until the two images converge. Second, rotations, constructed by presenting a series of projections constructed from different angles, are presented at the website http://renal.nephrology.iupui.edu/phillipsetal. Third, animations constructed with the IVIE real-time rendering software may also be found on this website. This software is capable of rendering 3-D volumes at rates of 4 to 8 frames per second, permitting an investigator to interactively evaluate an image volume by using a mouse to "grab" and manipulate the volume. Although the animations presented here do not allow interactive inspection of image volumes, the experience can be approximated by manipulating the movie progress bar after the animation has been completely downloaded from our website. Readers for whom stereoscopic viewing is difficult or impossible are encouraged to view the website animations.

Two-Photon Microscopy of Embryonic Mouse Kidneys

Two-photon microscopy allowed us to clearly visualize kidney development as the ureteric bud progressively invades the undifferentiated mesenchyme. Figure 1A shows no apparent differentiation of mesenchyme in 11½-day-old embryos (E11.5) labeled with PNA. By 13½ days, the primitive, symmetrical branches of the ureteric bud become apparent in tissue labeled with either PNA (Figure 1B) or SBA (Figure 1C). Whereas PNA predominantly labeled basolateral aspects of these early tubules, SBA strongly labeled lumenal and intracellular structures.

By 17½ days, the developing tubules are more numerous, extensive, and complex. At this point, PNA labels dichotomous branches extending from the maturing collecting system (Figure 2, A and B). The ampullae, or widened tips of the ureteric buds, appear to project outward like tree limbs. While these branching tubules were brightly labeled with PNA, particularly on the lumenal membranes, a dimmer, more uniform basal labeling was also seen in an intricate network of tubules throughout the volume (Figure 2, A and B, especially apparent in the

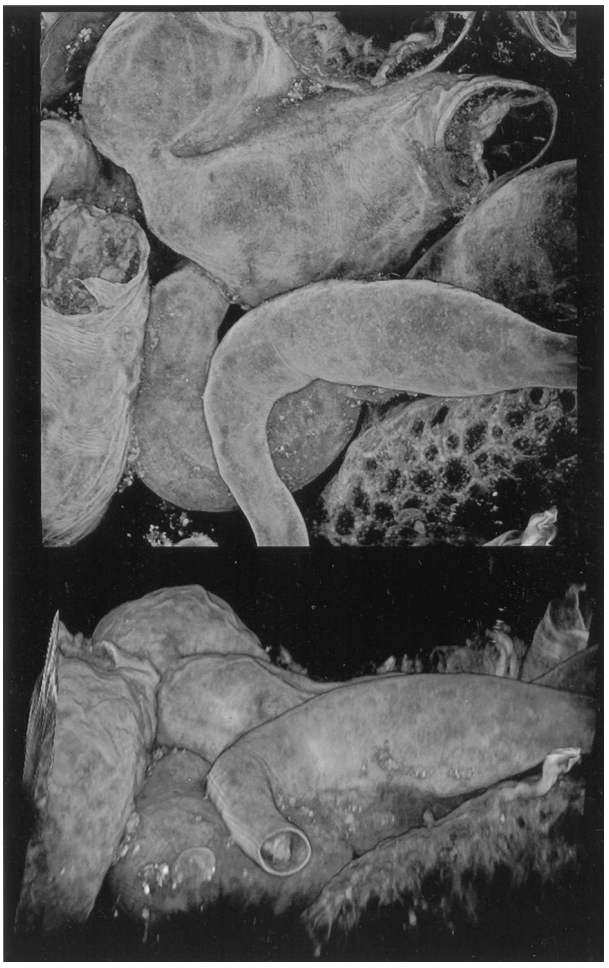

Figure 4. Renderings of the image volume of *inv/inv* kidneys shown in Figure 3C. Cysts arising from proximal tubules and a collecting duct are seen. The two perspectives shown here were produced using a voxel rendering program that performs real-time 3-D reprojection imaging (see Methods).

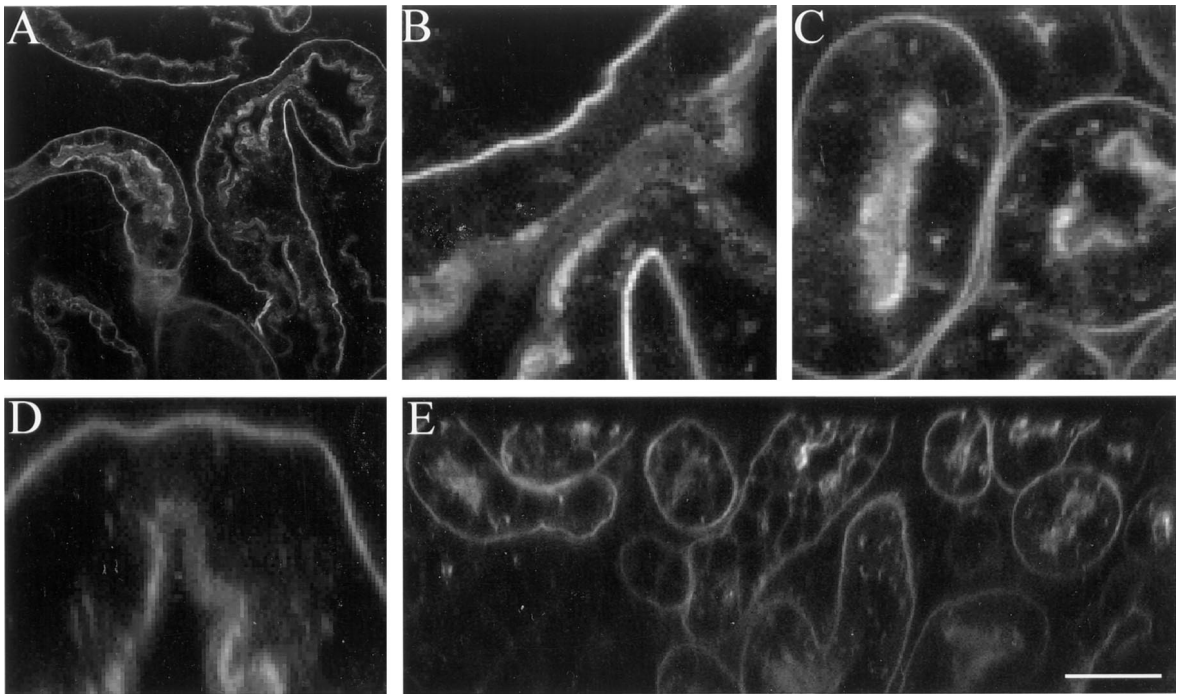

Figure 5. Resolution and contrast in two-photon microscopy. **A:** A single optical section from the 3-D volume shown in Figures 3C and 4 collected at a depth of 50 μm into the tissue. **B:** A magnified portion of this image (**A**) demonstrates the high resolution and contrast of the 2-photon images. **C:** A high magnification optical section taken from the image volume shown in Figure 3B, collected at a depth of 17 μm into the tissue. **D:** A high magnification image of a single vertical section from the image volume shown in Figure 3C. **E:** A vertical section of the image volume shown in Figure 3B. Scale bar, 50 μm (**A**), 10 μm (**B–D**), and 25 μm (**E**).

rotations). Some of these dimmer tubules are distal connecting segments of the developing nephron that link the nephrons to the ampullae of the collecting ducts. PNA staining of more mature collecting ducts, distinguished by the checkerboard pattern of intensely staining intercalated cells alternating with the more numerous but weakly staining principal cells, is also seen (right margin of Figure 2B and animated rotations of Figure 2, A and B). The relationship of these tubules is best viewed using the animated rotations (http://renal.nephrology.iupui.edu/phillipsetal). F-actin, labeled with fluorescent phalloidin, imparts a lace-like quality to reconstructed cross-sections of E17.5 tubules (Figure 2C). Defined F-actin staining is seen along the apical and basolateral aspects of cells comprising the ureteric bud. A ring of metanephric condensation is interposed between the stroma and ureteric bud.

Two-Photon Microscopy of Newborn Mouse Kidneys

When normal newborn (day P5) mouse kidneys were stained with LCA and imaged by two-photon microscopy, two glomeruli were seen to hang like berries from afferent arterioles (Figure 3A). An interlobular artery is also observed branching perpendicularly from a thick-walled arcuate artery running diagonally across the bottom of the micrograph. At this same time point, PNA labels a dense network of uniform tubules (Figure 3B). Waves of intensely staining apical brush borders flow along the lumenal aspect of convoluted proximal tubules stained with either LCA (Figure 3A) or PNA (Figure 3B). Interposed between proximal tubules are collecting ducts with intense lumenal labeling of intercalated cells (Figure 3B).

A strikingly different morphology is found in PNA-labeled cystic kidneys of day P5 transgenic *inv/inv* mice. These mice display a developmental symmetry disorder[16] but also provide a polycystic kidney model.[17,18] In contrast to the uniform tubules of age-matched wild-type mice (Figure 2B), cystic kidneys stained with PNA showed fusiform dilatation of proximal tubules and focal wrinkles along angles of an otherwise smooth basal surface (Figure 3C). Continuity between two cysts, bridged by a segment of normal caliber, may be seen in Figure 3C (right side). This continuous network of dilated and constricted tubules is consistent with that described for other mouse models of PKD[19,20] but is in contrast to morphology proposed by others, in which pouches and blind sacs are observed to extend from tubules.[21] As the cysts progressively expand, the epithelial cells flatten and, in the case of proximal tubules, show focal loss of apical brush border labeling. In contrast to normal kidneys, PNA showed the most intense staining along the basal membranes of cystic proximal tubules, but also stained apical membranes and intracellular vesicles of cystic collecting ducts (bottom left of Figure 3C). The image volumes shown in Figure 3C were rendered using the IVIE software to emphasize surface contours of cysts in two proximal tubules and one collecting duct (Figure 4, two perspectives). Close inspection of basal membranes of proximal tubules reveals geographic features such as wrinkles along angles, fibril-like bands, and tenting, the

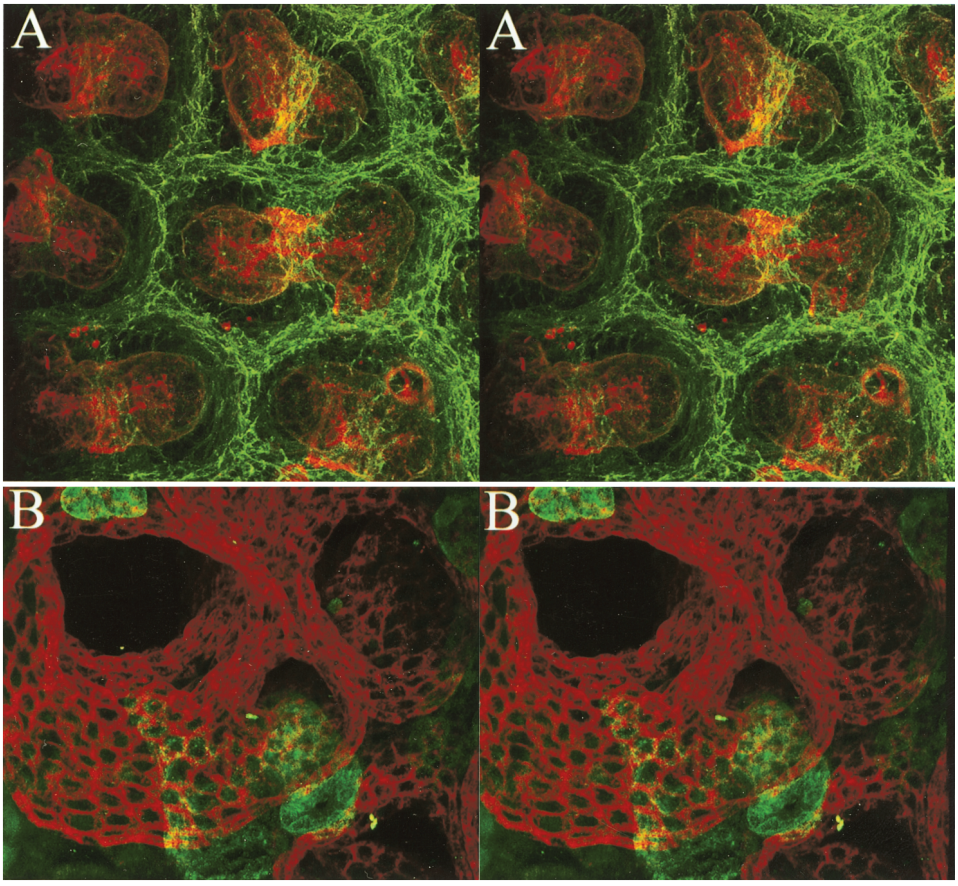

Figure 6. Stereopairs of dual-fluorochrome-labeled mouse renal tubules. Normal E17.5 (**A**) and P5 *inv/inv* (**B**) mouse kidneys were dual-labeled with rhodamine and fluorescein. In **A**, branches of ureteric bud (red) stained with PNA-rhodamine are separated by a network of mesenchyme stained with LCA-fluorescein (green). In **B**, cystic renal tubules labeled with DBA-rhodamine (red) are seen in close proximity to more normal caliber thick ascending loop of Henle labeled with anti-Tamm-Horsfall-fluorescein (green). Each image is 205 μm across. **A** shows projections collected over a depth of 68 μm and **B** a depth of 52 μm.

last of which may be a fixation artifact. This detailed topography, based on the binding pattern of a single lectin, rivals the morphology visualized by low-power scanning electron microscopy.

Resolution and Contrast in Two-Photon Microscopy

An example of a single optical section from the 3-D volumes shown in Figures 3C and 4 is shown in Figure 5A. This image was collected 72 microns into the kidney. A magnified portion of this image (Figure 5B) demonstrates the high resolution and contrast of the two-photon images. The resolution of these images is reflected in the image of the tubule margin, which is a single pixel (0.44 μm) across. A comparable image taken from the image volume of the normal kidney shown in Figure 3B is shown in Figure 5C. Again the tubule margin is imaged in sharp detail. In both figures, PNA can be seen labeling the basal aspects of the tubules as well as the brush border membranes of the tubule lumen. As pointed out in Figure 3, the basal membranes appear to be more intensely labeled in tubules of the *inv/inv* mice (Figure 5B) than in tubules of control littermates (Figure 5C).

The vertical resolution of this technique can be assessed in vertical sections reconstructed from the stack of horizontal optical sections of the original image volumes. Figure 5D shows a high magnification image of a single vertical section from the image volume shown in Figure 3C. Although the tubule edges are still sharply defined, vertical resolution is perhaps 2 to 3 times worse than horizontal resolution. One of the chief advantages of two-photon microscopy is its ability to collect images deep in labeled samples. The extended imaging capability is apparent in Figure 5E, which is a vertical section of the image volume shown in Figure 3B. High contrast and sharp definition is apparent throughout the 130-μm depth of this image volume.

Multiparameter Two-Photon Microscopy

Fluorescence microscopy offers the ability to characterize the distribution of multiple structures or multiple molecules in the same image volume. Whereas two-photon microscopy is currently limited to the use of a single wavelength of light to stimulate fluorescence, the physics of two-photon fluorescence is such that a single wavelength of light is capable of efficiently exciting chromatically distinct fluorophores. Examples of multicolor two-photon microscopy are shown in Figure 6.

Figure 6A shows an image volume of a 17½-day-old embryonic kidney labeled with both fluorescein-conjugated LCA and rhodamine-conjugated PNA. A network of undifferentiated mesenchyme labeled with LCA (green)

separates ampullae of ureteric bud preferentially labeled with PNA (red).

Figure 6B shows an image volume of a newborn (P5) *inv/inv* mouse kidney labeled with rhodamine-DBA and a fluorescein-conjugated secondary antibody directed against a primary antibody to Tamm-Horsfall protein. In the *inv/inv* kidneys, the distended collecting ducts labeled with DBA (red) are clearly distinguished from more normal-appearing thick ascending loops of Henle labeled with anti-Tamm-Horsfall antibody (green).

Discussion

The recent confluence of advances in microscopy, digital image processing, and genetics has provided a fertile field for the study of development. The approach used in the present study combined two-photon microscopy, advanced 3-D image analysis, and genetic manipulation. This combination provides a powerful tool for characterizing complex 3-D structures, particularly for organogenesis studies of both normal and pathological processes in animal models. For example, this approach provides for rapid assessment of the histopathological defects after transgene mutations. Additionally, using fluorescently conjugated antibodies, one can also characterize the expression of functionally important proteins.

The morphology of nephrogenesis has been advanced by the exhaustive work of a number of investigators, including the microdissections of Oliver[22] and Osathanondh and Potter.[9–13] In her classic text of kidney development, the pathologist Edith Louise Potter noted, these "studies have been anatomical, and no attempt has been made to follow the establishment of function."[21] In this study of 3-D imaging technology, we demonstrate the advantages of using two-photon microscopy for rendering the complex *in situ* tissue architecture of developing mouse kidney while simultaneously labeling specific molecules that are important to understanding renal function.

Compared with laser confocal microscopy, two-photon excitation provides superior deep imaging with minimal bleaching of fluorochromes. Full-thickness visualization was possible in tissue sections cut from 40 to 180 μm in thickness. Two-photon microscopy and advanced 3-D image analysis provided relatively rapid and detailed morphological information when tissue sections were stained with fluorescently labeled phalloidin, lectins, or antibody. Such an approach will help to identify the molecular pathways of normal and pathological development.

Acknowledgments

We thank Exing Wang for expert technical assistance and Vincent Gattone for his careful reading of the manuscript.

References

1. Inoue S: Foundations of confocal scanned imaging in light microscopy. Handbook of Biological Microscopy. Edited by Pawley JB. New York, Plenum Press, 1995, pp 1–17
2. Keller HE: Objective lenses for confocal microscopy. Handbook of Biological Microscopy. Edited by Pawley JB. New York, Plenum Press, 1995, pp 111–126
3. Dunn KW, Wang E: Optical aberrations and objective choice in multicolor confocal microscopy. Biotechniques 2000, 28:542–550
4. Denk W, Piston DW, Webb WW: Two-photon molecular excitation in laser-scanning microscopy. Handbook of Biological Confocal Microscopy. Edited by Pawley JB. New York, Plenum Press, 1995, pp 445–458
5. Davies JA, Bard JBL: Inductive interactions between mesenchyme and the ureteric bud. Exp Nephrol 1996, 4:77–85
6. Huber C: On the development and shape of uriniferous tubules of certain higher mammals. Am J Anat Suppl 1905, 4:1–98
7. Ludwig E: Uber Frühstadien der menschlichen Ureterbaumes. Acta Anat 1962, 49:168–185
8. Evan AP, Gattone VH 2d, Blomgren PM: Application of scanning electron microscopy to kidney development and nephron maturation. Scan Electron Microsc 1984 (Pt 1):455–473
9. Osathanondh V, Potter EL: Development of human kidney as shown by microdissection. I. Arch Pathol 1963, 76:271–276
10. Osathanondh V, Potter EL: Development of human kidney as shown by microdissection. II. Arch Pathol 1963, 76:277–289
11. Osathanondh V, Potter EL: Development of human kidney as shown by microdissection. III. Arch Pathol 1963, 76:290–302
12. Osathanondh V, Potter EL: Development of human kidney as shown by microdissection. IV. Development of tubular portions of nephrons. Arch Pathol 1966, 82:391–402
13. Osathanondh V, Potter EL: Development of human kidney as shown by microdissection. V. Development of vascular pattern of glomerulus. Arch Pathol 1966, 82:403–411
14. Laitinen L, Virtanen I, Saxen L: Changes in the glycosylation pattern during embryonic development of mouse kidney as revealed with lectin conjugates. J Histochem Cytochem 1987, 35:55–65
15. Ronco P, Brunisholz M, Richet G: Pathophysiologic aspects of THP: a phylogenetically conserved marker for the thick ascending limb of Henle's loop. Adv Nephrol 1987, 16:253–256
16. Yokoyama T, Copeland NG, Jenkins NA, Montgomery CA, Elder FF, Overbeek PA: Reversal of left-right asymmetry: a situs inversus mutation. Science 1993, 260:679–682
17. Mochizuki T, Saijoh Y, Tsuchiya K, Shirayoshi Y, Takai S, Taya C, Yonekawa H, Yamada K, Nihei H, Nakatsuji N, Overbeek PA, Hamada H, and Yokoyama T: Cloning of *inv*, a gene that controls left/right asymmetry and kidney development. Nature 1998, 395:177–181
18. Morgan D, Turnpenny L, Goodship J, Dai W, Majumder K, Matthews L, Gardner A, Schuster G, Vien L, Harrison W, Elder FF, Penman-Splitt M, Overbeek P, Strachan T: Inversin, a novel gene in the vertebrate left-right axis pathway, is partially deleted in the inv mouse. Nat Genet 1998, 20:149–156
19. Avner ED, Studnicki FE, Young MC, Sweeney WE Jr, Piesco NP, Ellis D, Fettermann GH: Congenital murine polycystic kidney disease. I. The ontogeny of tubular cyst formation. Pediatr Nephrol 1987, 1:587–596
20. Gattone VH 2d, Calvet JP, Cowley BD Jr, Evan AP, Shaver TS, Helmstadter K, Grantham JJ: Autosomal recessive polycystic kidney disease in a murine model: a gross and microscopic description. Lab Invest 1988, 59:231–238
21. Potter EL: Normal and Abnormal Development of the Kidney. Chicago, Year Book Medical Publishers, Inc., 1972, pp 124–130, vii-viii
22. Oliver J: Nephrons and Kidneys. New York, Hoeber Medical Division, Harper & Row, 1968, plates I-XXV